Title:	Computational material design for energy and gas storage applications
Author(s):	Gonzales, Ivana
Intended for:	University of New Mexico, School of Engineering seminar, 18th February, 2013

Los Alamos
NATIONAL LABORATORY
—— EST. 1943 ——

Computational material design for energy and gas storage applications

Ivana Gonzales

Physics and Chemistry of Materials

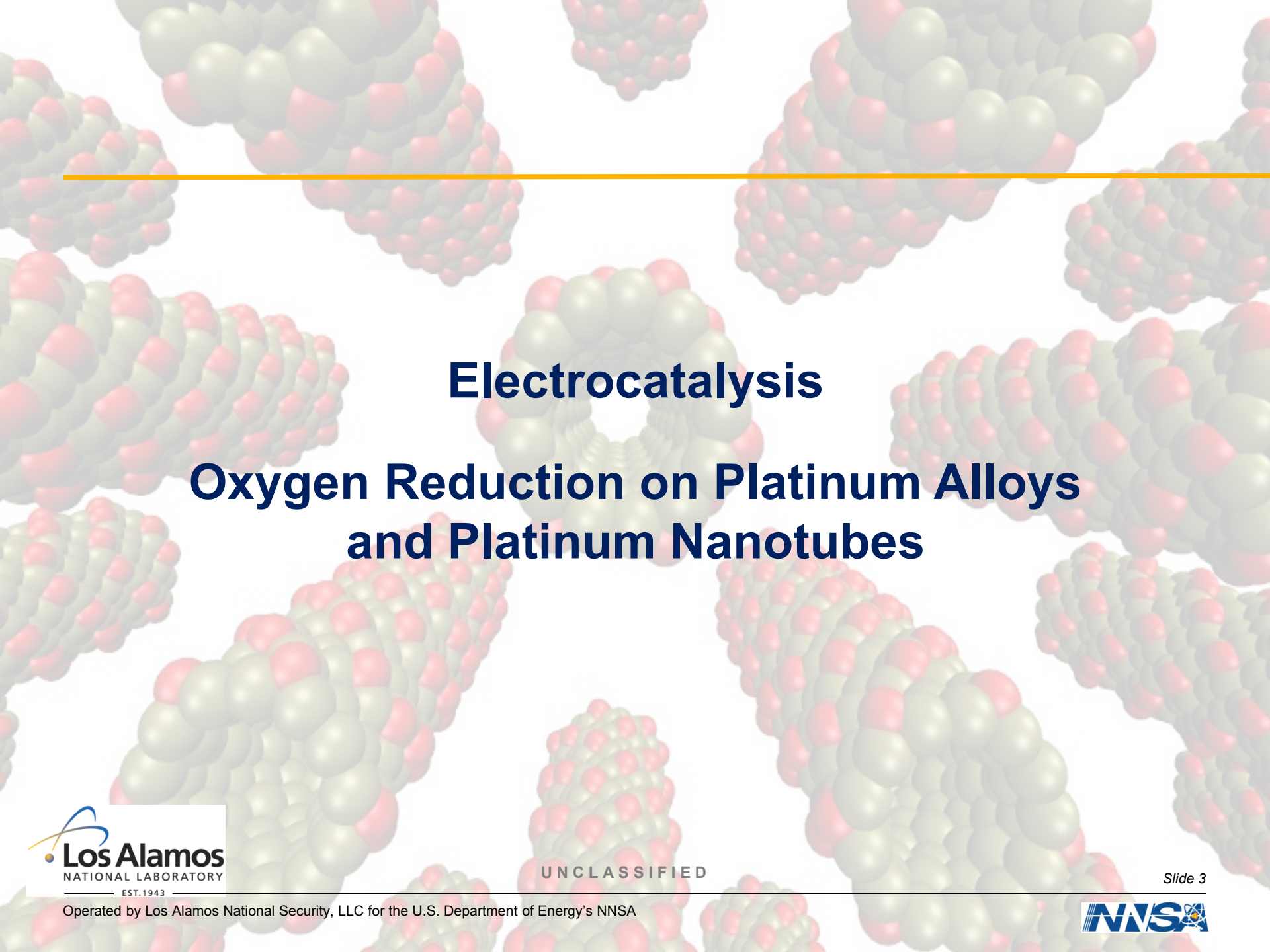**Los Alamos National Laboratory (LANL)**

Los Alamos, USA

UNM, February 2013

Overview

Energy Storage in Chemical Bonds:

- Electrocatalytic reduction of oxygen on platinum alloys and nanostructures

- Electrocatalytic reduction of nitrogen on molybdenum nitride

Hydrogen Storage in Metal Organic Frameworks

Electrocatalysis

Oxygen Reduction on Platinum Alloys and Platinum Nanotubes

Introduction

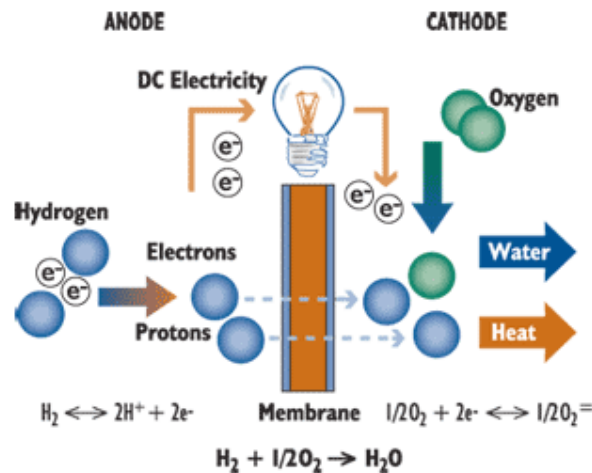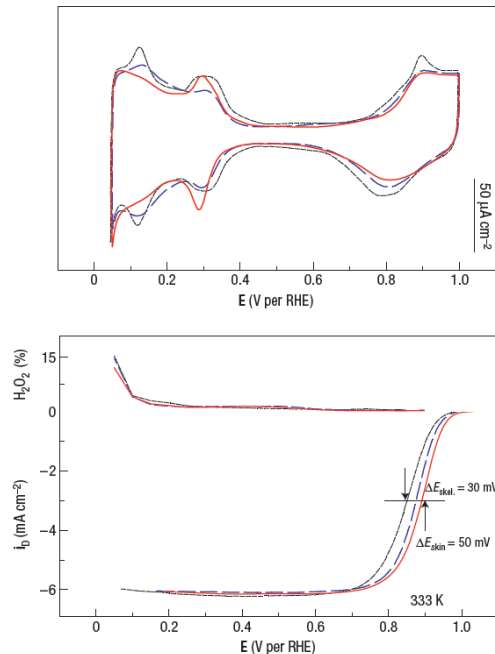Fuel cells have a potential for highly efficient use of chemical fuels, compared to heat engines

Figure: hydrogen/oxygen fuel cell

Operated by Los Alamos National Security, LLC for the U.S. Department of Energy's NNSA

Introduction

slow kinetics of the oxygen reduction reaction (ORR) in acidic environment

$$O_2(g, 1atm) + 4e^- + 4H^+(aq, 1M) \rightarrow 2H_2O \quad E^0_{half\_cell} = 1.23V$$

significant cathode overpotential decreases the fuel cell electrical efficiency:

overpotential of 500-600 meV - efficiency of 45-55 % compared to the theoretical thermodynamic efficiency of 93 % at 25 ℃.

$$\Delta_r G_{cell} = -nF\Delta E_{cell}$$

Figure: Cyclic voltammograms and polarization curve of ORR on Pt₃Fe

Motivation

Reducing the ORR overpotential / cost:
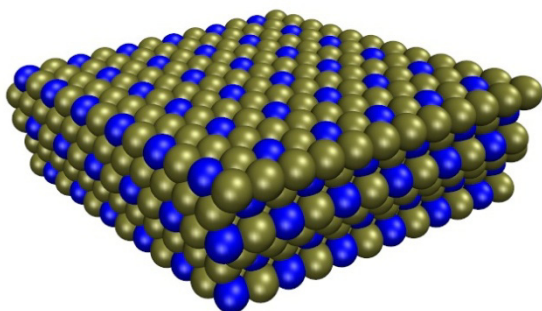
(1) alloying platinum with platinum group metals

(2) nanostructures: nanotubes and nanoparticles

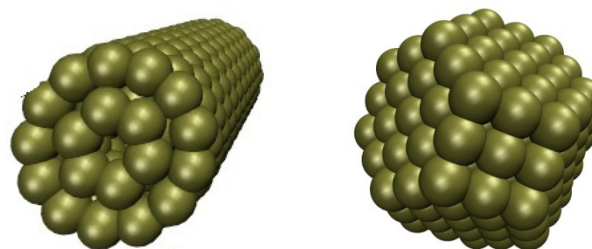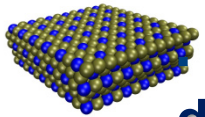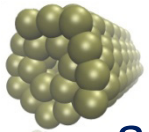**Figure: Pt$_3$Ni(111) surface**

Figure: (6,6)@(13,13) MWPtNT nanotube and 2nm Pt$_{201}$ cluster
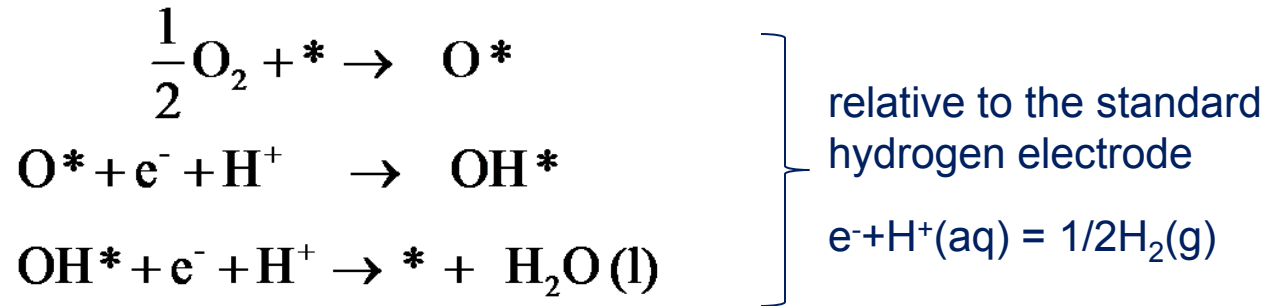
Motivation

study the influence of alloying component **concentration and distribution** on the **ORR activity** and **stability** in aqueous environment

study the effect of **size and structure** of a nanomaterial on the ORR activity and stability in aqueous environment

Methodology - study of ORR mechanism

Reactions connecting different states of the metal surface(*) in the ORR mechanism

$$\frac{1}{2}O_2 + * \rightarrow O*$$

$$O* + e^- + H^+ \rightarrow OH*$$

$$OH* + e^- + H^+ \rightarrow * + H_2O\,(l)$$

relative to the standard hydrogen electrode

$e^- + H^+(aq) = 1/2H_2(g)$

Free gibbs energy of the reactions

$$\Delta G_{w,water} = \Delta E_{w,water} + \Delta ZPE + T\Delta S$$

$$\Delta G(U, pH, T = 298\,K) = \Delta G_{w,water} - eU + kT\ln(10)pH$$

bias effect

correction for the free energy of H+

Technical details

- VASP program

- DFT with PAW method using GGA approximation with PW91, PBE and RPBE exchange-correlation terms

- 3 layer $2\sqrt{3} \times 2\sqrt{3}$ (111) slab with 13.5 Å vacuum layer

- effect of solvent – bilayer of water molecules on the surface

- 4 x 4 x 1 k-point Monkhorst-Pack mesh

- plane-wave basis with a cutoff energy of 400 eV

- Methfessel-Paxton smearing of order 2 with sigma value of 0.2 eV
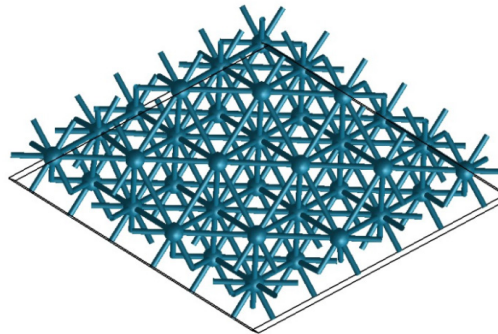
Oxygen Reduction Reaction: Energetics

Table: The binding Enthalpies and Free energy changes at U=0 V and pH=0 for different absorbents with water on Pt surfaces with different concentration of Ni in a second layer (1/3 coverage)

		OH* + $e^- + H^+$	O* + $2(e^- + H^+)$	H* - $e^- + H^+$
Pt(111)	$\Delta E_{w,water}$	0.45 eV	1.43 eV	-0.38 eV
	$\Delta G_{w,water}$	0.80 eV	1.48 eV	-0.14 eV
	U_f	0.8 V	0.74 V	0.14 V
Pt$_3$Ni(111)seg	$\Delta E_{w,water}$	0.74 eV	2.04 eV	-0.16 eV
	$\Delta G_{w,water}$	1.09 eV	2.09 eV	0.08 eV
	U_f	1.1 V	1.40 V	-0.08 V
PtNi(111)seg	$\Delta E_{w,water}$	0.97 eV	2.34 eV	-0.01 eV
	$\Delta G_{w,water}$	1.32 eV	2.39 eV	0.23 eV
	U_f	1.32 V	1.20 V	-0.23 V
PtNi$_3$(111) seg	$\Delta E_{w,water}$	1.05 eV	2.43 eV	0.10 eV
	$\Delta G_{w,water}$	1.40 eV	2.48 eV	0.34 eV
	U_f	1.4 V	1.24 V	-0.34 V
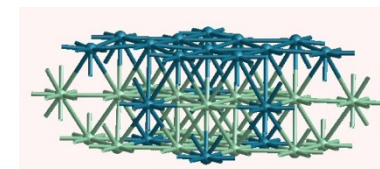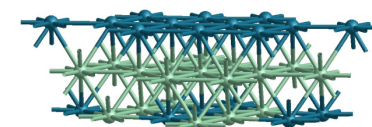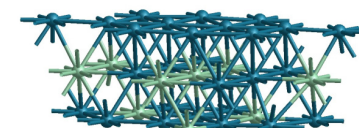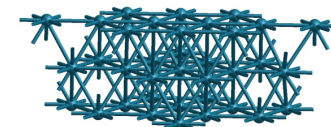
Oxygen Reduction Reaction: Free energy diagrams

$$\frac{1}{2}O_2 + * \rightarrow O*$$ (1)

$$O* + e^- + H^+ \rightarrow OH*$$ (2)

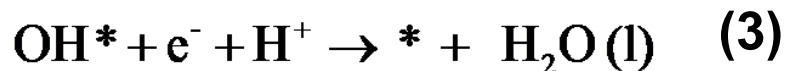$$OH* + e^- + H^+ \rightarrow * + H_2O\,(l)$$ (3)
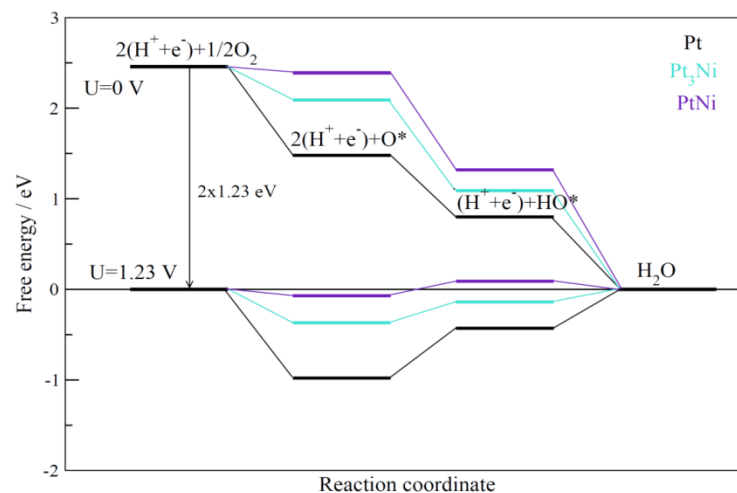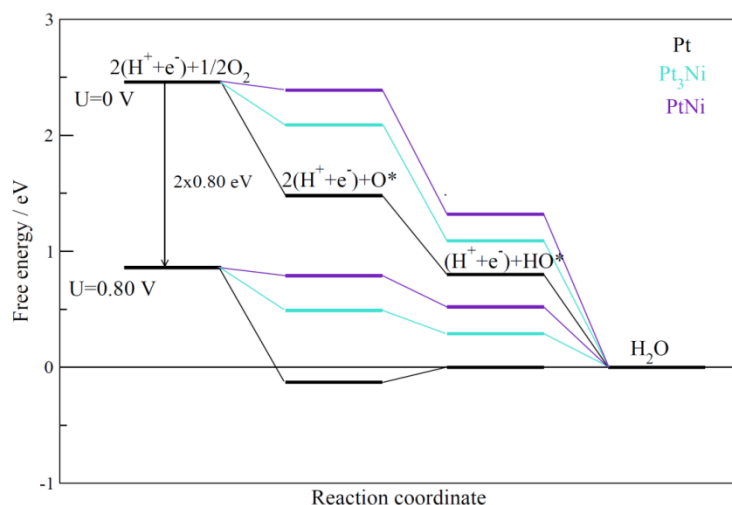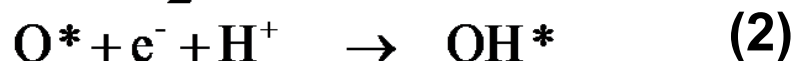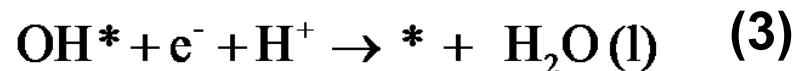

Figure: Free-energy diagrams for ORR over Pt(111) surfaces with different Ni concentration in the second layer, for cell potentials U=0.80 V and U=1.23 V

Oxygen Reduction Reaction: Free energy diagrams

$$\frac{1}{2}O_2 + * \rightarrow O*$$ (1)

$$O* + e^- + H^+ \rightarrow OH*$$ (2)

$$OH* + e^- + H^+ \rightarrow * + H_2O \, (l)$$ (3)
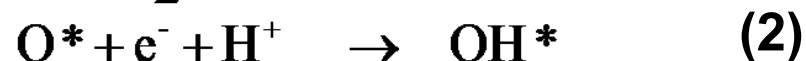
estimated catalytic activity:

$$Pt < Pt_3Ni < PtNi_3 < PtNi$$

550 > 240 > 190 > 150 mV

confirmed experimentally:

Y. Liu et al, J. Phys. Chem. C, 116, 7848 (2012)

M. Karpenter, JACS, 134, 8535 (2012)

Stability of the surfaces

Estimate of the shift in the electrochemical dissolution potential

Table: surface cohesive energy and the estimate of the shift in the electrochemical dissolution potential relative to Pt(111)

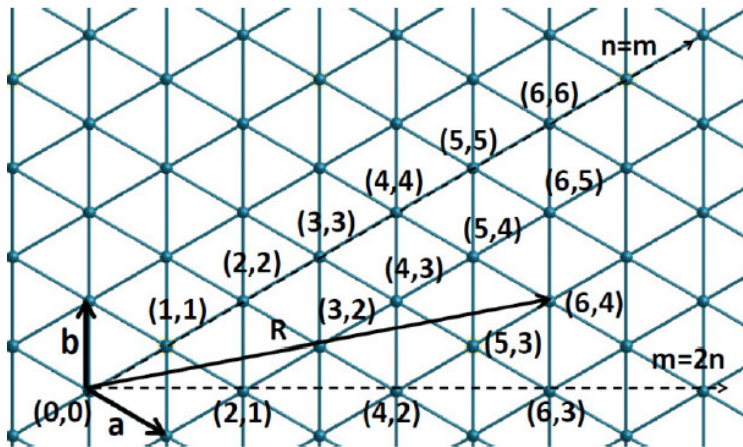| reaction	$M_N(\text{surface}) \rightarrow$ $M_{N-1} + M$	$\Delta E/eV$	$\Delta U_{\text{corr}}/V$	$\Delta U_{\text{corr}}^{b}/V$
Pt(111)		5.79	0.00	0.00
Pt$_3$Ni(111)	site 1	6.11		
	site 2	6.23		
	site 3	6.04	+0.13	+0.10
PtNi(111)	site 1	6.41		
	site 2	6.38	+0.30	+0.30
PtNi$_3$(111)	site 1	5.69		
	site 2	5.58	−0.11	−0.23

PtNi$_3$

- more susceptible to electrochemical dissolution of Pt monolayer

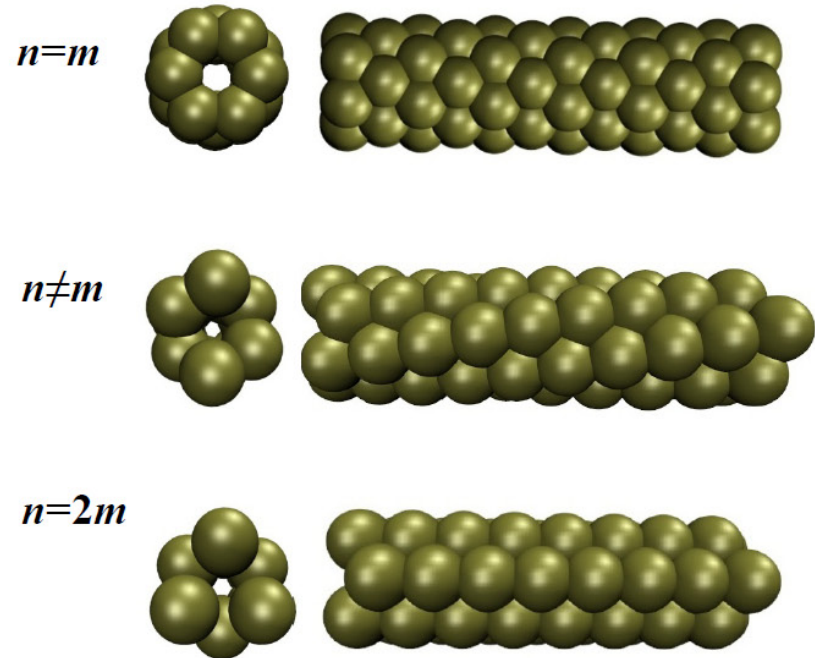- more susceptible to poisoning of the surface by the formation of nickel oxide

I. Matanovic et al. J. Phys. Chem. C, 115, 10640 (2011)

UNCLASSIFIED

Operated by Los Alamos National Security, LLC for the U.S. Department of Energy's NNSA

Pt nanotubes

PtNT: Rolling-up Pt(111) sheet to form a tube
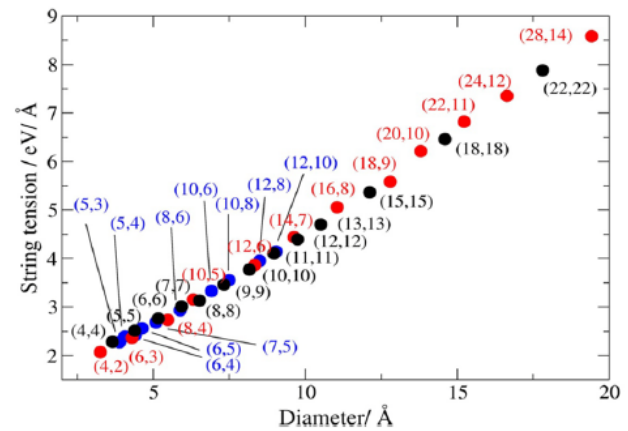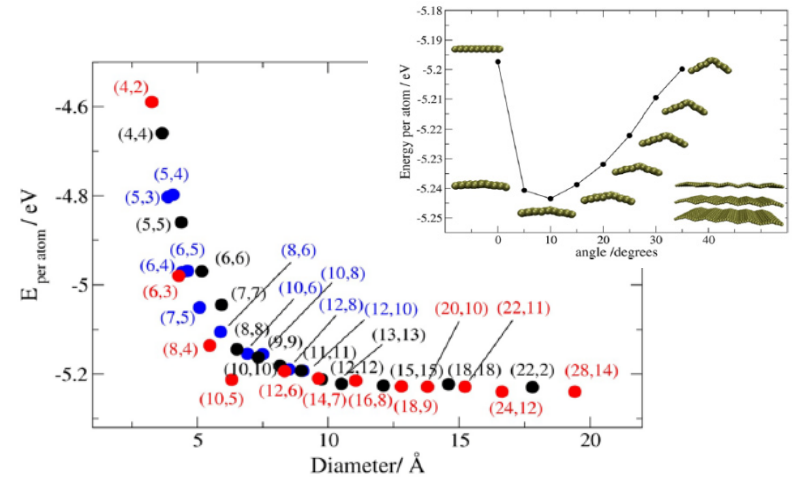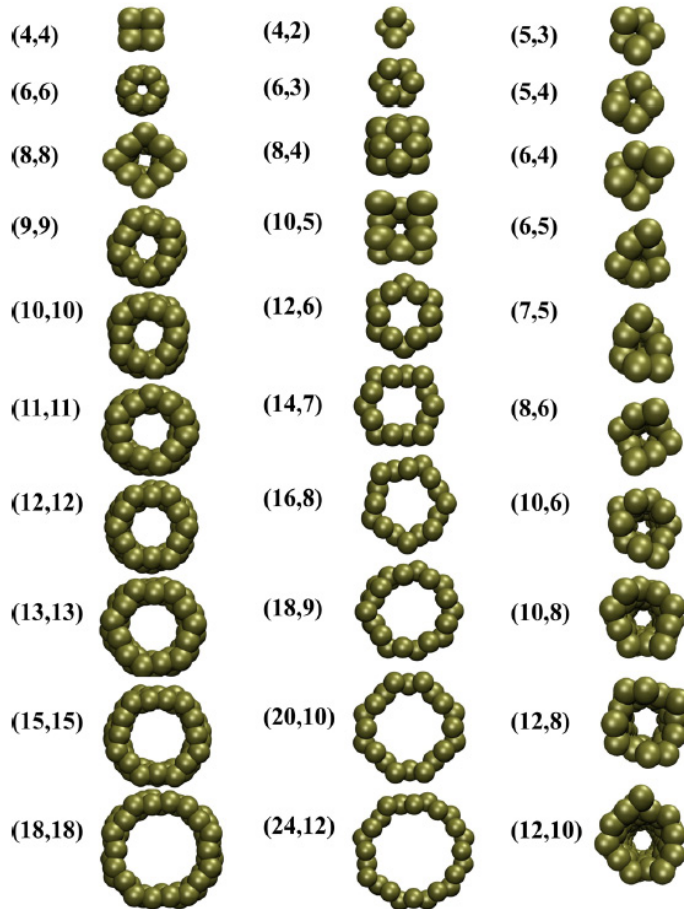

rolling vector: $R = na + mb$

$$r = \frac{\sqrt{2}a_c}{4\pi}\sqrt{n^2 + m^2 - nm}$$

a_c = 3.70- 3.85 Å

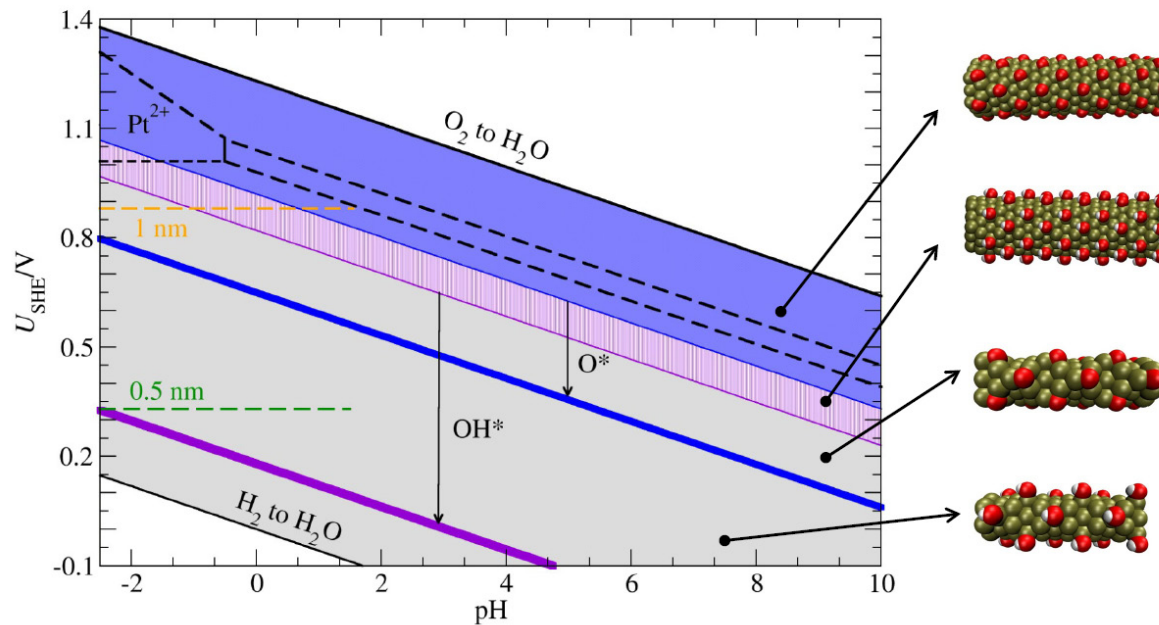# Pt nanotubes

Pourbaix diagrams

Figure: Calculated surface Pourbaix diagrams for Pt nanotubes compared to a bulk Pourbaix diagrams (black dashed lines)

Dissociative oxygen reduction reaction (ORR) mechanism

$$\frac{1}{2}O_2 + * \rightarrow O*$$

$$O* + e^- + H^+ \rightarrow OH*$$

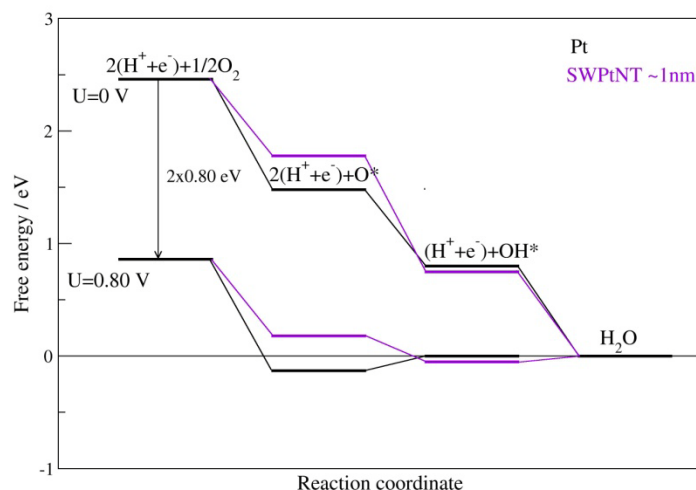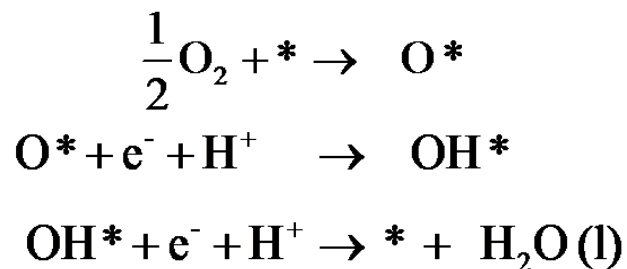$$OH* + e^- + H^+ \rightarrow * + H_2O\,(l)$$

Figure: Free-energy diagrams for ORR over Pt(111) surfaces and SWPtNT for cell potentials U=0.80 V

PtNTs, d ~ 1nm

smaller ORR overpotential than Pt(111), up to 100 meV

Pt nanotubes – ab initio MD simulations in water

Aim (1) characterize change of atomic and electronic structure on solvation

(2) structure of water around curved surfaces - water-surface interface models
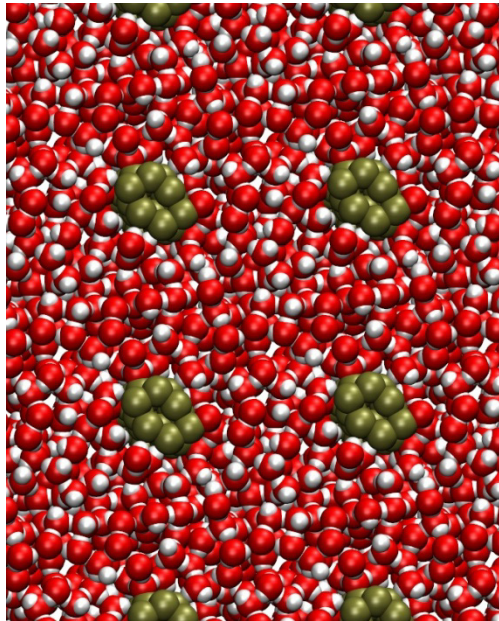
(6,6) and   **(13,13) SWPtNT in water**

~800 atom cell, 1300 MD steps in 24h, 480 processors, average ~1min/step

Conclusions
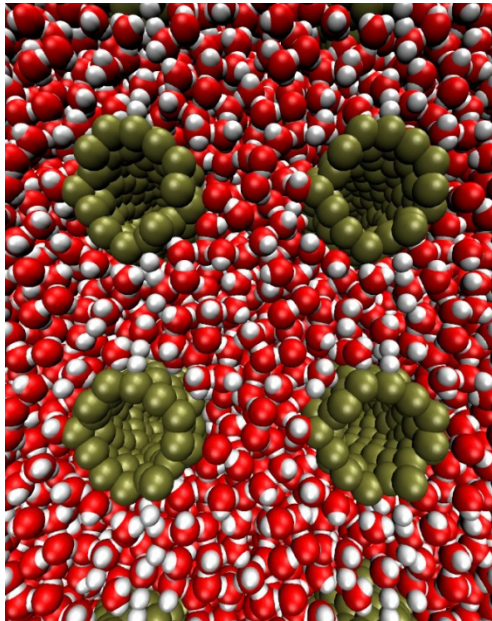
▪ catalytic activity – modification in the electronic structure induced by the specific subsurface composition

The ORR overpotential was found to decrease :

$$Pt < Pt_3Ni < PtNi_3 < PtNi$$

Oxygen reduction reaction on Pt-Ni alloys

$$2H^+ + 2e^- + 1/2O_2 \rightarrow H_2O$$
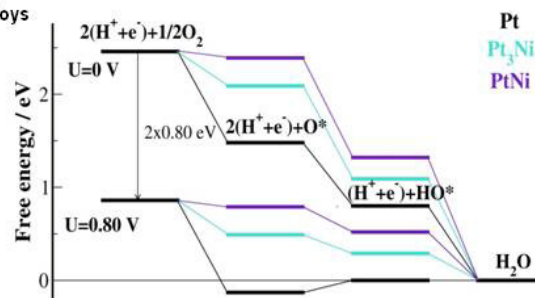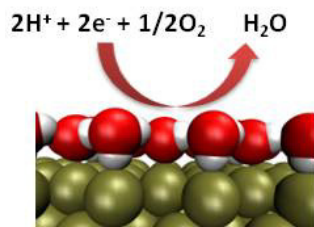
▪ shifts in the electrochemical dissolution potentials relative to Pt indicate that PtNi is the least susceptible to corrosion

Operated by Los Alamos National Security, LLC for the U.S. Department of Energy's NNSA

Conclusions

- ~0.5 nm nanotubes bind oxygen/hydroxyl more strongly than Pt(111)

  ~1 nm nanotubes bind oxygen/hydroxyl comparable or weaker than Pt(111)
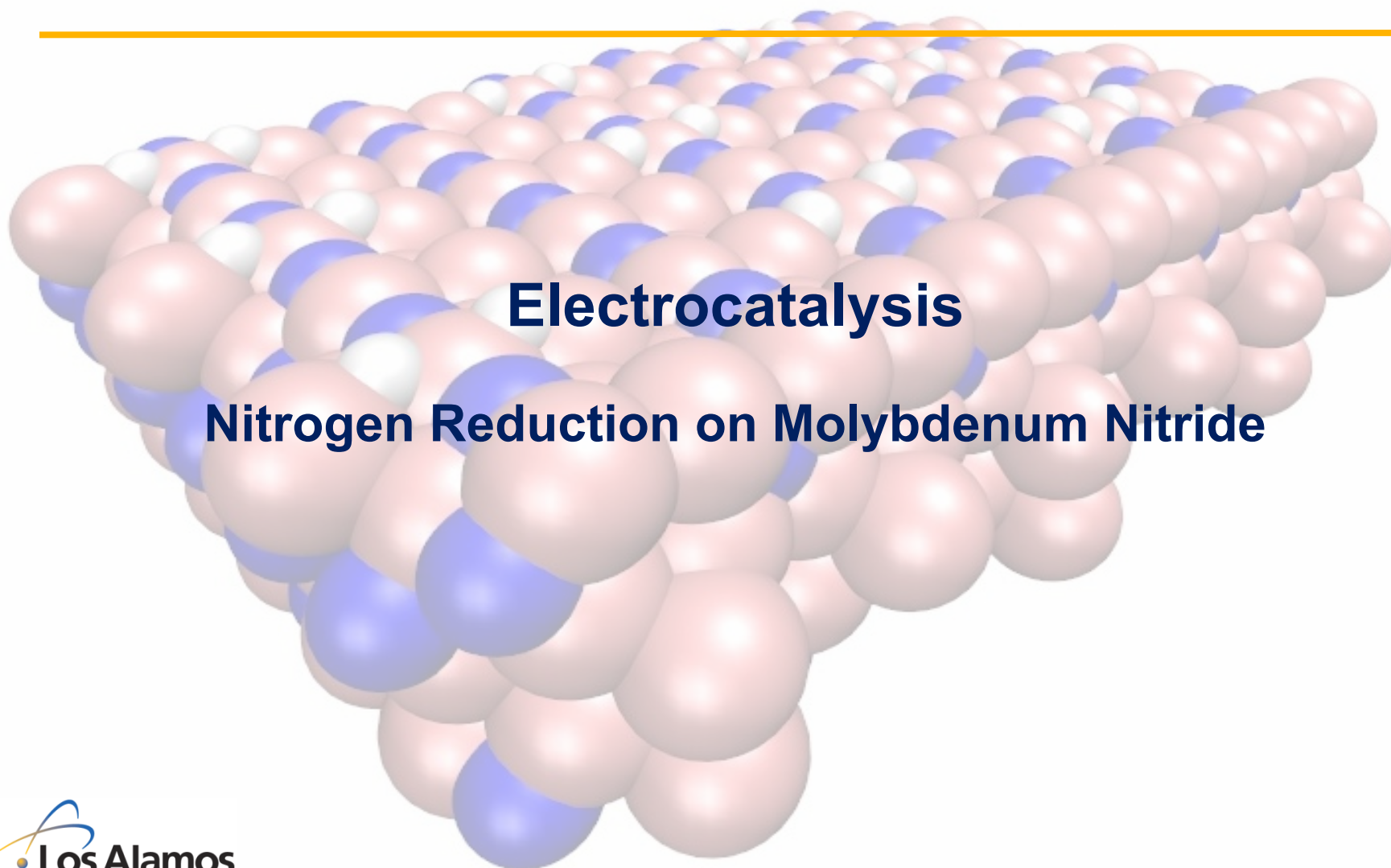
  reduced ORR overpotential – SWPtNT with a diameter > 1nm

- control size/chirality – fine tuning of reactivity → separation of metal nanotubes by geometric specification or size

- all studied nanotubes more susceptible to electrochemical dissolution than Pt(111) – potential corrosion problem

I. Matanovic et al. J. Phys. Chem. C, 116, 16499 (2012)

I. Matanovic et al, J. Electrochem. Soc, submitted

Los Alamos
NATIONAL LABORATORY
EST.1943

U N C L A S S I F I E D

Slide 20

Operated by Los Alamos National Security, LLC for the U.S. Department of Energy's NNSA

Electrocatalysis

Nitrogen Reduction on Molybdenum Nitride

Electro-reduction of nitrogen

- ammonia can be obtained by electro-reduction of nitrogen

$$N_2 + 6e^- + 6H^+ \rightarrow 2NH_3$$
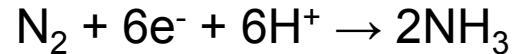
protons are supplied from electro-oxidation of hydrogen or water

Marnellos et al. Science 282 (5386) 98-100

Holbrook and Ganley, US patent 7811442 (2010):
electrochemical synthesis of ammonia using high temperature proton
conductors at atmospheric pressures
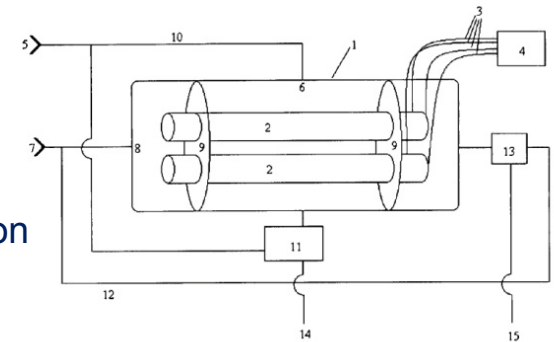
- challenges: development, characterization and optimization of **new electrocatalyists** for ammonia electrosythesis and stable anhydrous **proton conducting electrolytes**

Introduction

- early transition metal nitrides - possible replacements for platinum-group metal catalysts
- demonstrated catalytic activity for isomerisation, dehydrogenation, hydrogenation, water gas shift and amination reactions with competitive rates

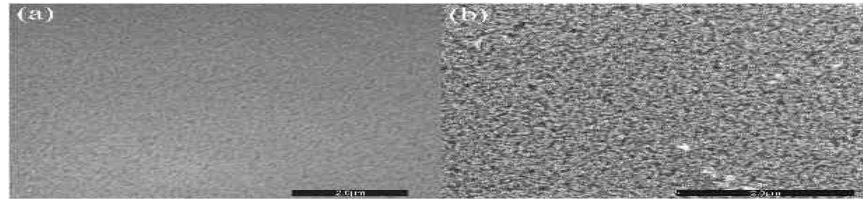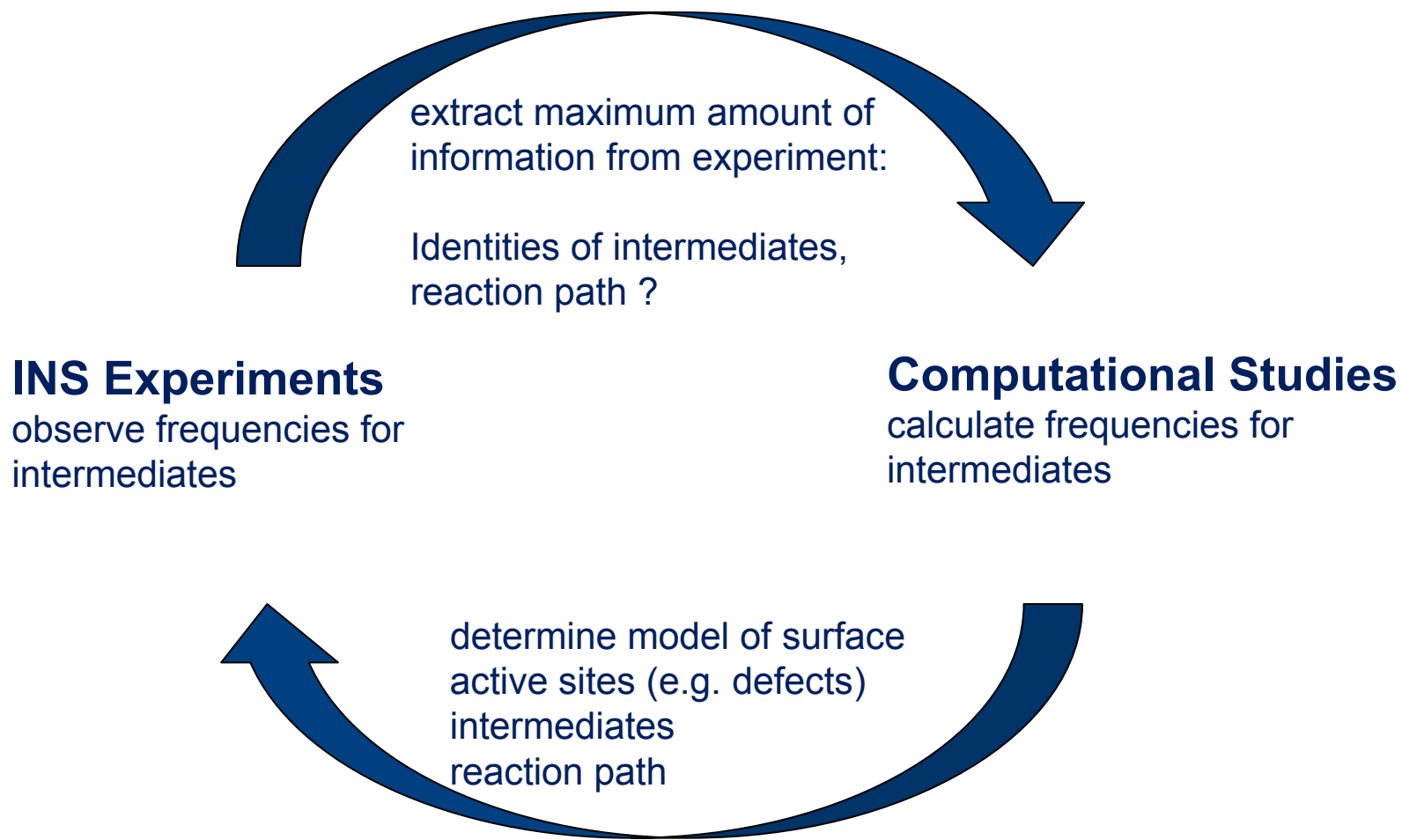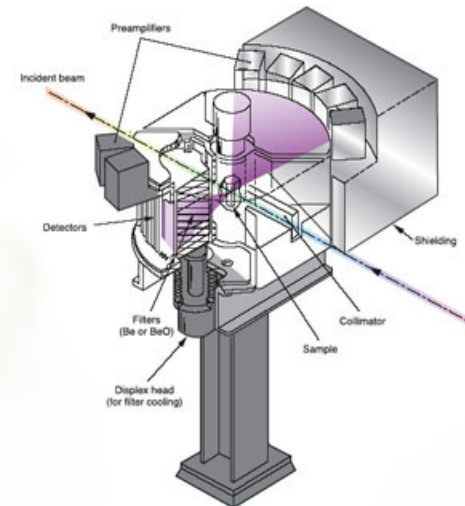Mo_2N – high surface area films synthesized at LANL (polymer assisted deposition)

Figure: Field emission scanning electron microscope (FESEM) images

Synergy of Inelastic Neutron Scattering and Computation: Ammonia synthesis on novel material

extract maximum amount of information from experiment:

Identities of intermediates, reaction path ?

INS Experiments
observe frequencies for intermediates

Computational Studies
calculate frequencies for intermediates

determine model of surface active sites (e.g. defects) intermediates reaction path

Inelastic neutron scattering experiment

The Filter Difference Spectrometer (FDS) at LANL

- used for molecular vibrational spectroscopy by **inelastic neutron scattering**
- most useful for measurements requiring high sensitivity; for example, very dilute systems or molecules adsorbed on surfaces such as in catalysts

vibrational spectra measured on FDS

- < 1g sample of catalyst adsorb in-situ H_2, then add N_2

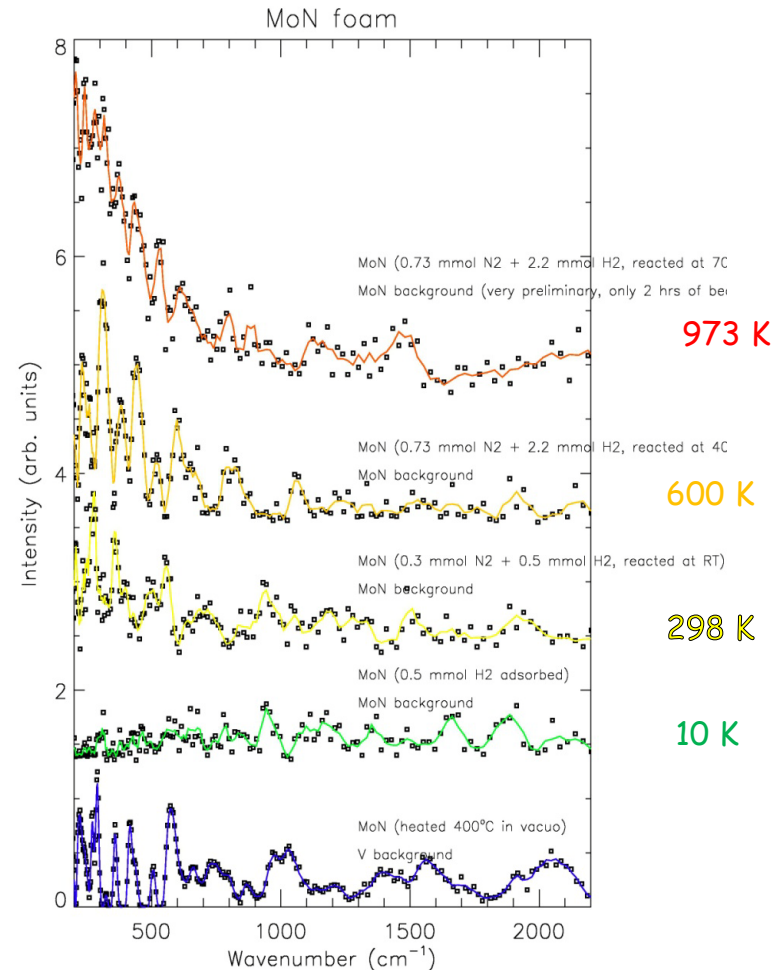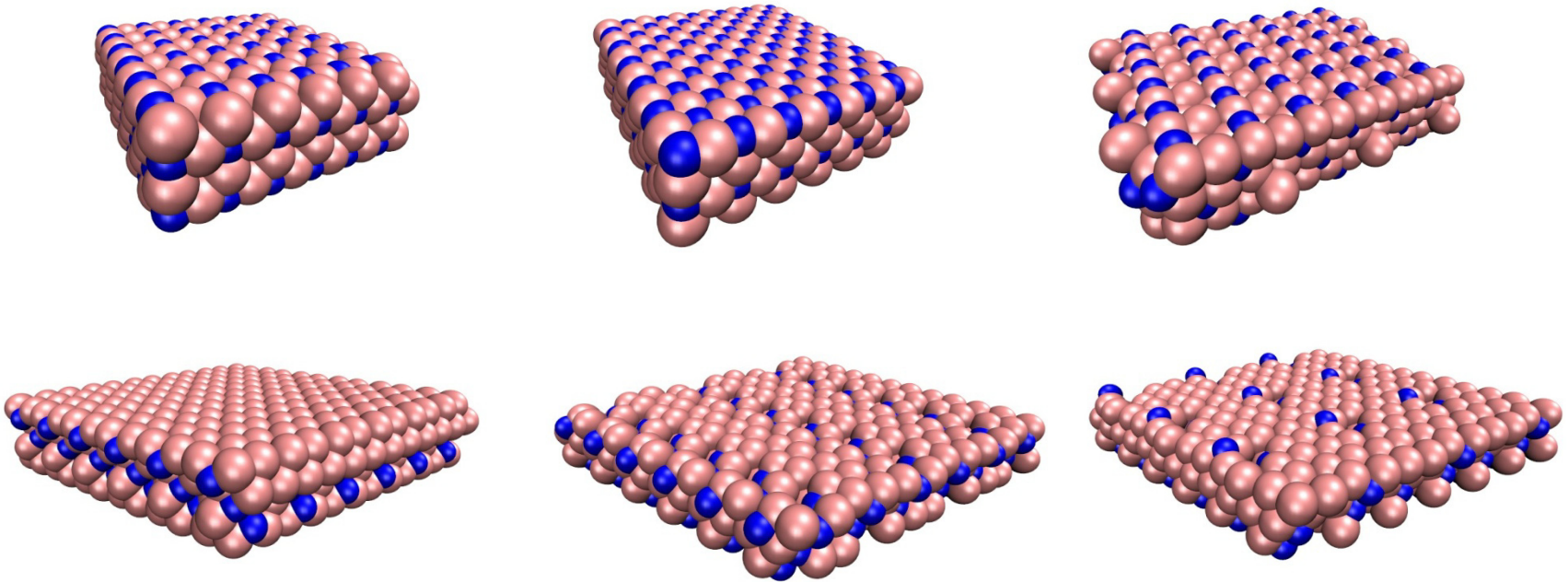- heat stepwise to increasing T

- collect INS spectrum at each step

MoN foam

973 K
600 K
298 K
10 K

Figure: INS spectra of reactive species on MoN

Ammonia synthesis on novel MoN material

- model the surface

- model the reaction on the surface – identify the intermediates

- model the INS spectra – compare with the experiment

reactivity of γ-Mo$_2$N towards hydrogen

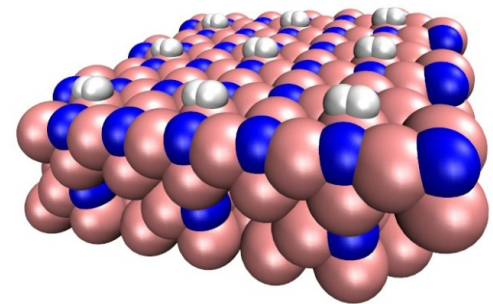|	(001)/eV	(100/010)/eV	(111)/eV	(111)*	(101)/eV
$\Delta E(\mathrm{H}_2)$	does not bind	-0.46	-0.81	dissociates	dissociates
$\Delta E(\mathrm{H})$ terminal1	-2.34	-2.53			
$\Delta E(\mathrm{H})$ terminal2		-2.40			
$\Delta E(\mathrm{H})$ bridging	-2.03	-2.69		-3.28	-3.80
$\Delta E(\mathrm{H})$ fcc			-3.48	-3.22	

∗ surface with defects introduced

different surfaces – very different reactivity: (001) does NOT adsorb H$_2$, (101) and (111) + defects dissociates H$_2$

molecular chemisorption (Kubas dihydrogen complex)

d(Mo-H$_2$) = 1.86 Å
d(H-H) = 0.85 Å (activated H-H bond)

reactivity of γ-Mo₂N towards hydrogen

	$(001)/\text{cm}^{-1}$	$(100/010)/\text{cm}^{-1}$	$(111)/\text{cm}^{-1}$	$(111)^*/\text{cm}^{-1}$	$(101)/\text{cm}^{-1}$
H terminal1	1745, 739	1732, 727			
H terminal2	n/a	1675, 731			
H bridging	1208, 910	829, 701		1280, 1157	1339, 1231
H fcc			1233, 951, 823	1260, 1013	

- intensities calculated from DFT vibrational frequencies ω_k and amplitudes C^k

incoherent cross section for atom i

double differential cross section

$$\frac{d^2\sigma}{d\Omega dE} = \frac{\mathbf{k}}{\mathbf{k}_0}\sum_i \frac{\sigma_i^{\text{inc}}}{4\pi} S_i^{inc}(\mathbf{Q},\omega)$$

$$S_i^{\text{inc}}(\mathbf{Q},\omega) = \exp(-Q^2\langle \mathbf{u}_i^2\rangle)\frac{\hbar|Q\cdot C_i^k|}{2\omega_k}\delta(\omega-\omega_k)$$

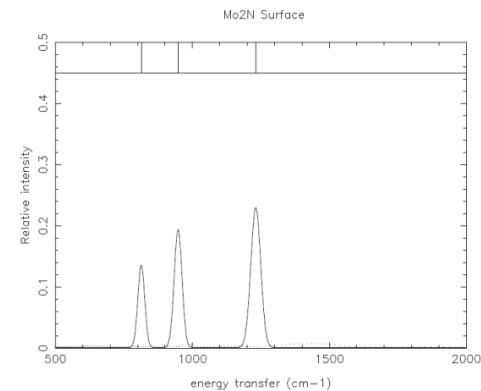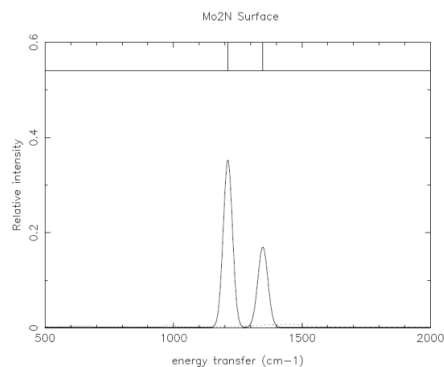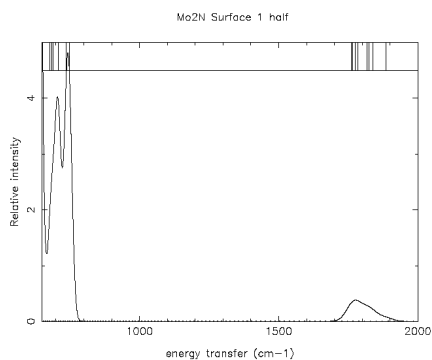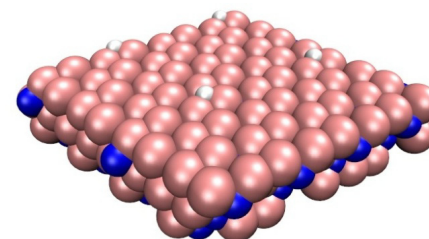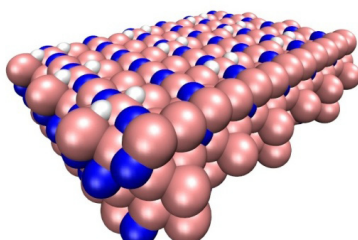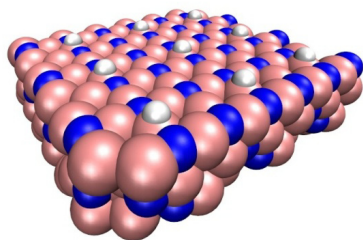momentum transfer
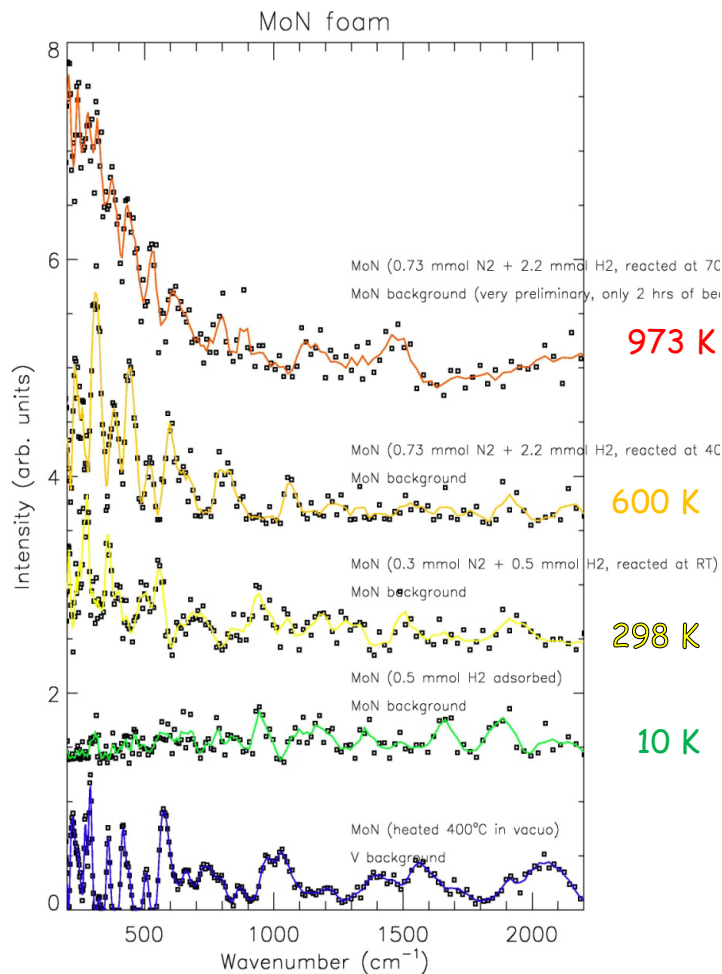experimental value: $\mathbf{Q} = \mathbf{k} - \mathbf{k}_0$

mean-square amplitude for atom i

reactivity of γ-Mo₂N towards hydrogen

	$(001)/\text{cm}^{-1}$	$(100/010)/\text{cm}^{-1}$	$(111)/\text{cm}^{-1}$	$(111)^*/\text{cm}^{-1}$	$(101)/\text{cm}^{-1}$
H terminal1	1745, 739	1732, 727			
H terminal2	n/a	1675, 731			
H bridging	1208, 910	829, 701		1280, 1157	1339, 1231
H fcc			1233, 951, 823	1260, 1013	

INS spectra assignment

Figure: INS spectra of reactive species on MoN

(10 K) fcc H: 950, 1250 cm^{-1}
 bridging H: ~ 600, ~800, 1140 cm^{-1}
 terminal H: ~700, 1645 cm^{-1}
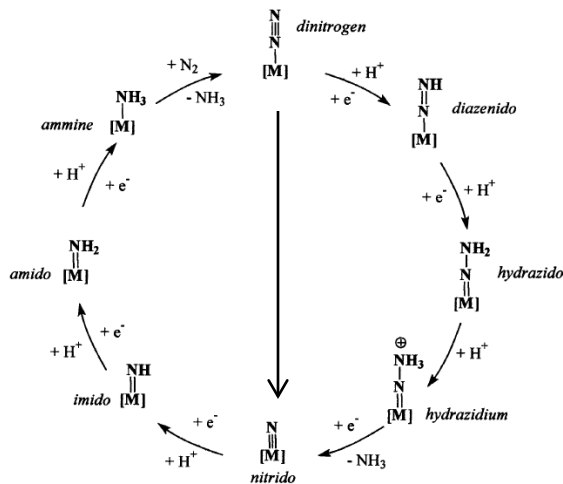
reactivity of γ-Mo₂N: adsorption energies

- DFT calculations used to estimate the free energy of each elementary step in ammonia sythesis

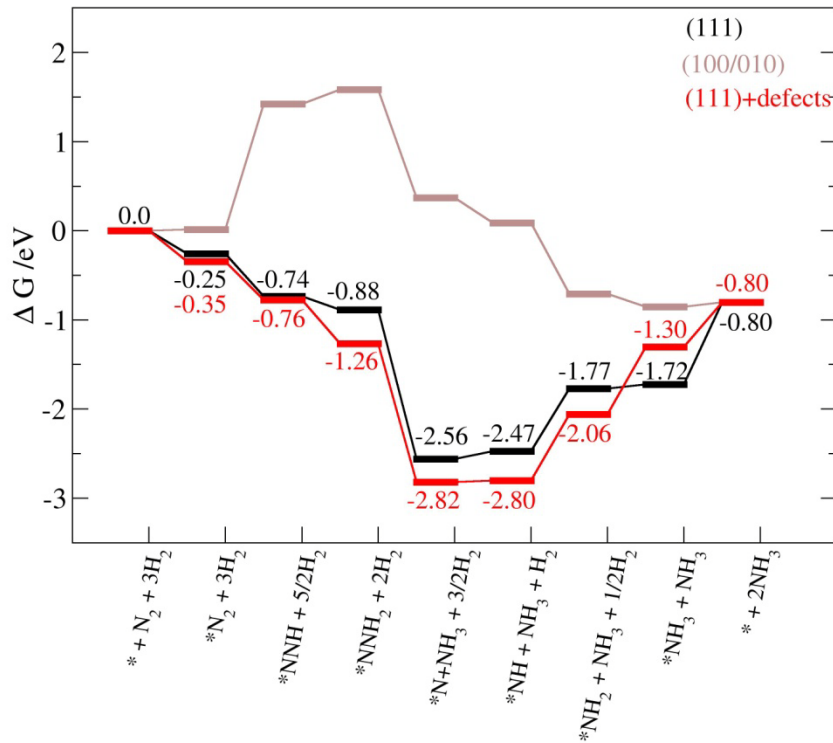$$\Delta G = \Delta E + \Delta E_{\text{ZPE}} + T\Delta S$$

|	$\Delta E_{(100/010)}$/eV	$\Delta E_{(111)}$/eV	$\Delta E_{(111*)}$/eV
N₂	-0.65	-0.92	-1.01
N	-4.88	-7.84	-8.07
NNH	-1.65	-2.42	-2.51
NNH₂	-2.94	-4.15	-4.34
NNH₃	-2.41	-4.17	-5.64
NH	-3.86	-6.42	-6.75
NH₂	-2.97	-4.03	-4.32
NH₃	-0.95	-1.82	-1.40

∗ surface with defects introduced

reactivity of γ-Mo$_2$N: energetics
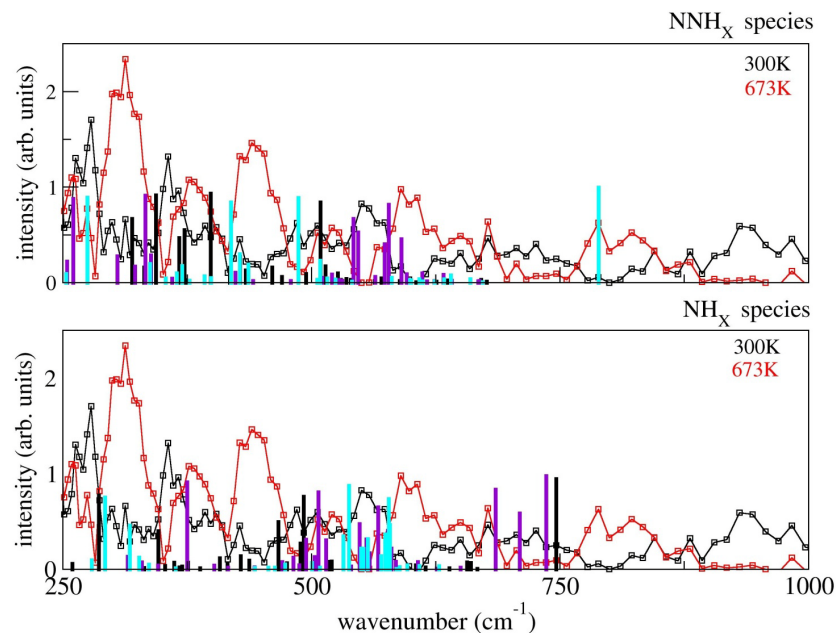
associative mechanism

dissociative mechanism

Operated by Los Alamos National Security, LLC for the U.S. Department of Energy's NNSA
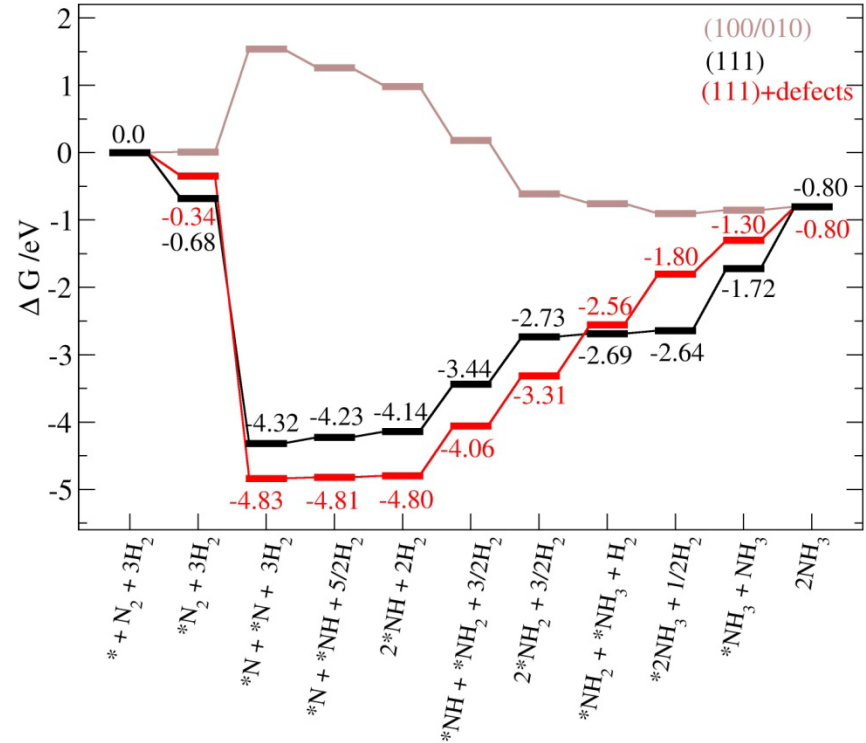
INS spectra: (111) perfect surface

(111) perfect surface
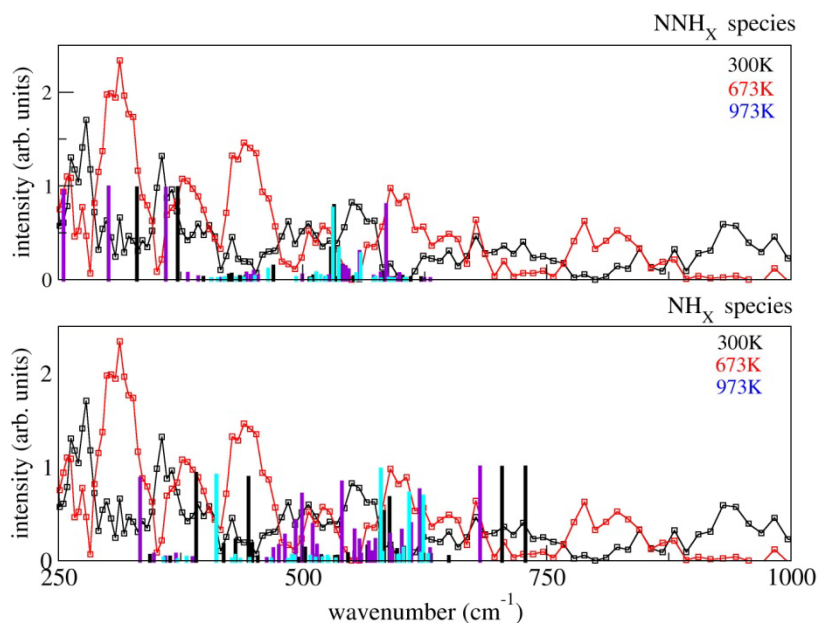
(111) surface with defects

assignment

Figure: INS spectra of reactive species on MoN
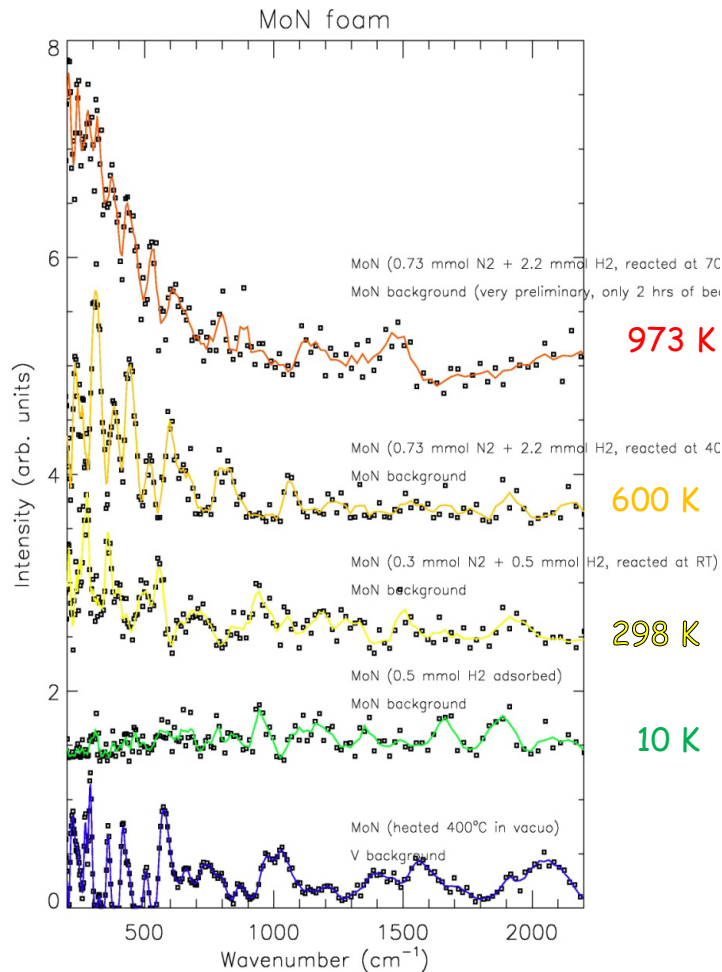
(973 K) NNH_x species gone; mainly NH_x species left.
ammonia phonon DOS states below 400 cm^{-1}
Mo-(NH_3) complex, incl. (NH_3) torsion at 120 cm^{-1} !!
Peaks at ~ 600, 800, 900, 1150 and 1475 cm^{-1}

(600 K) H species gone; peaks at 425, 510, 600, 660, 725,
1070, (weak: *1240*, *1550*), 1900 cm^{-1}:
mainly NNH and NNH_2;
plus more strong peaks below 400 cm^{-1}:

(298 K) Similar to (10 K), but fewer H species,
new peaks at ~500, 700 and 1550cm^{-1}: NNH

(10 K) fcc H: 950, 1250 cm^{-1}
bridging H: ~ 600, ~800, 1140 cm^{-1}
terminal H: ~700, 1645 cm^{-1}
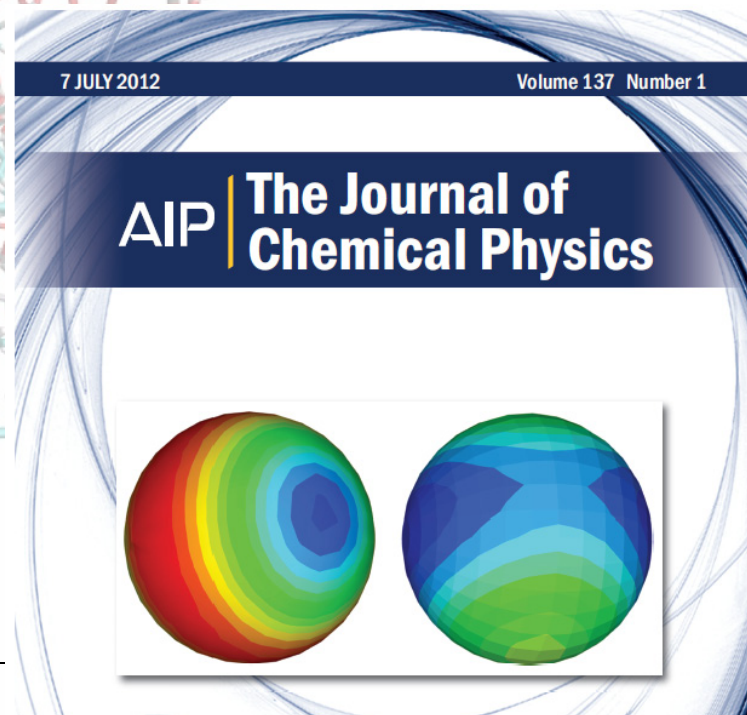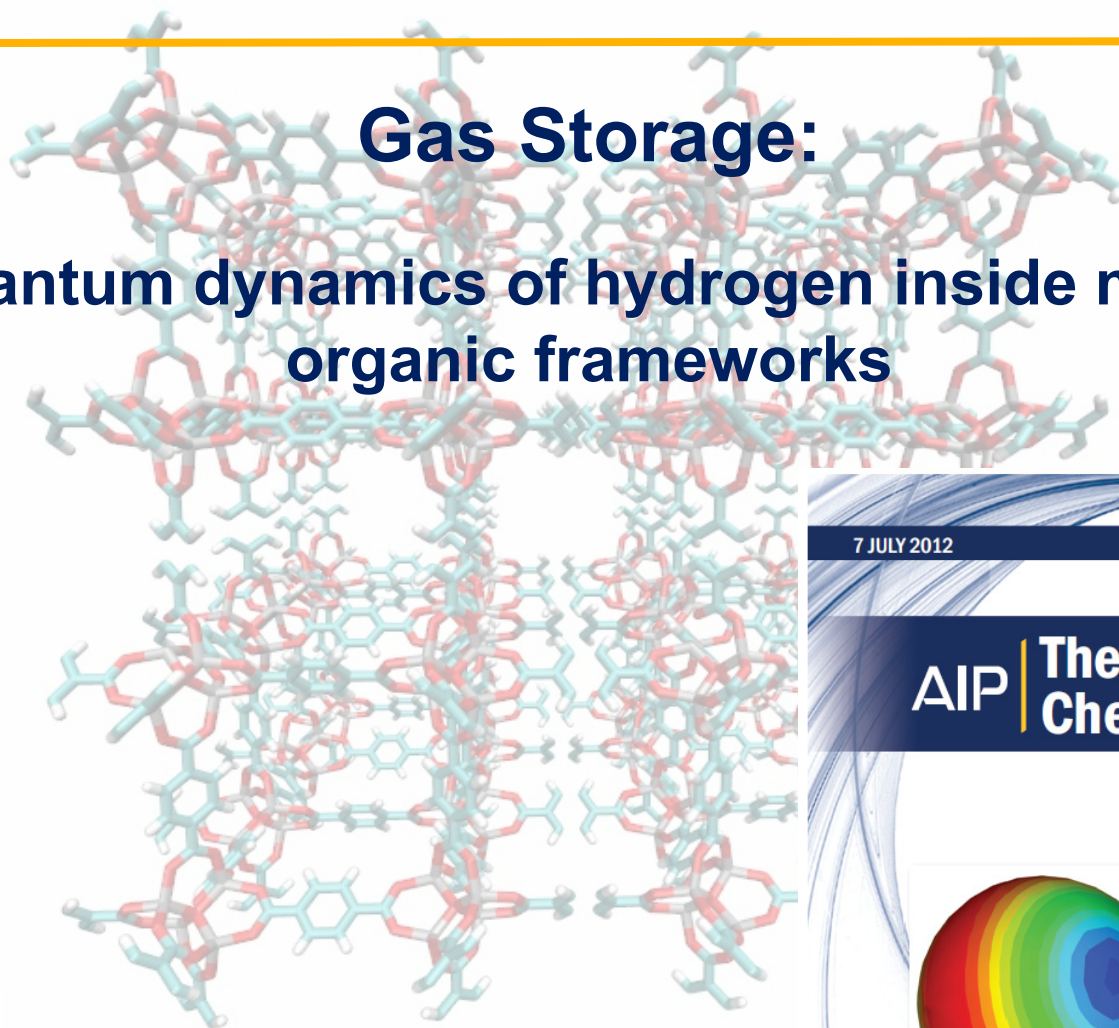
Conclusions

- we have investigated the catalytic mechanism and the active sites of newly synthesized material using inelastic scattering of neutrons and DFT calculations

- different surfaces have very different reactivity towards N_2, H_2 and NNH_x, NH_x species

- active sites: (111) defect sites with under-coordinated Mo
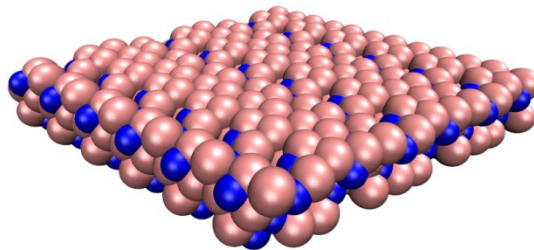
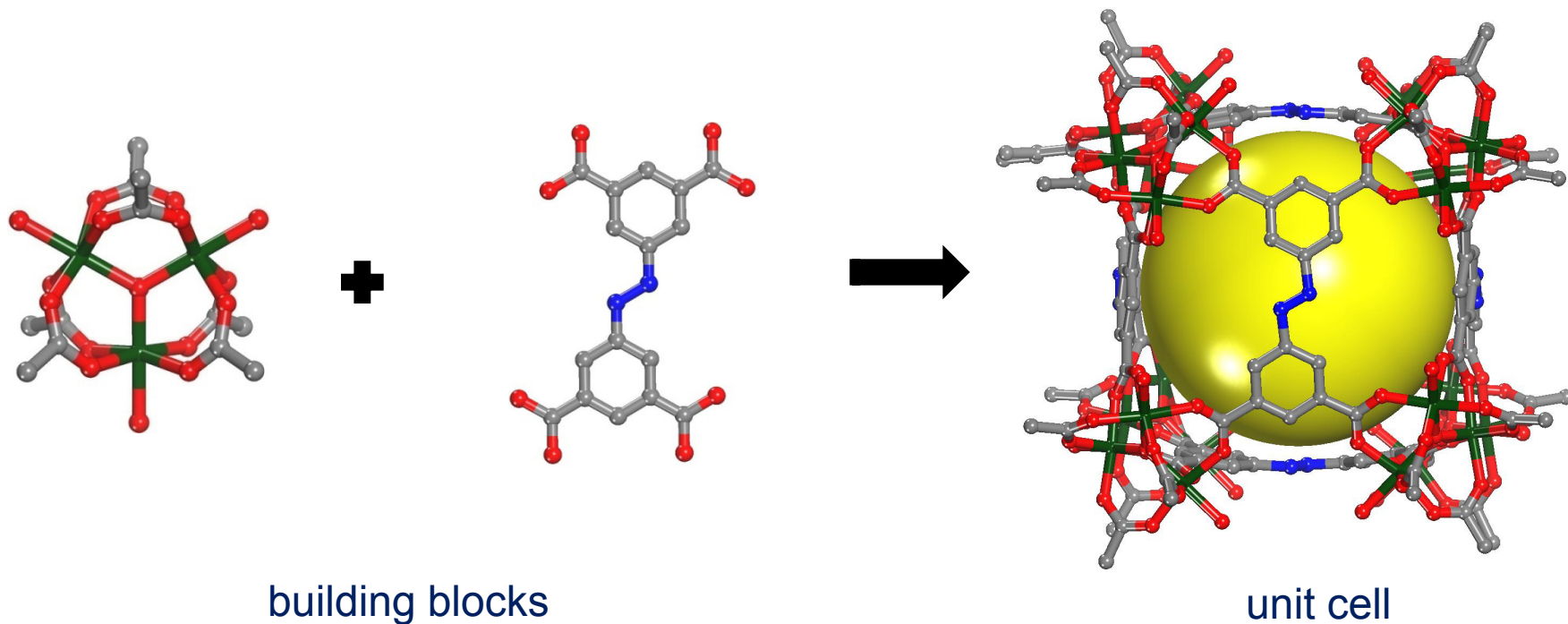- synthesis of ammonia proceeds through the formation of both NNH_x and NH_x species

Los Alamos
NATIONAL LABORATORY
EST.1943

Gas Storage:

Quantum dynamics of hydrogen inside metal-organic frameworks

Los Alamos
NATIONAL LABORATORY
EST.1943

Introduction

Metal organic frameworks (MOFs) - inorganic units connected with organic linkers

building blocks

unit cell

Los Alamos
NATIONAL LABORATORY
EST.1943

UNCLASSIFIED

Operated by Los Alamos National Security, LLC for the U.S. Department of Energy's NNSA

Slide 38

NNSA

Introduction

applications: gas storage and separation (H_2, CH_4, CO_2), catalysis

MOF -5 - close to the U.S. DOE requriements for on board hydrogen storage
     7.1 wt % but at 40 bar and 77K

$Zn_4O(1,4-benzenedicarboxylate)_3$

U N C L A S S I F I E D
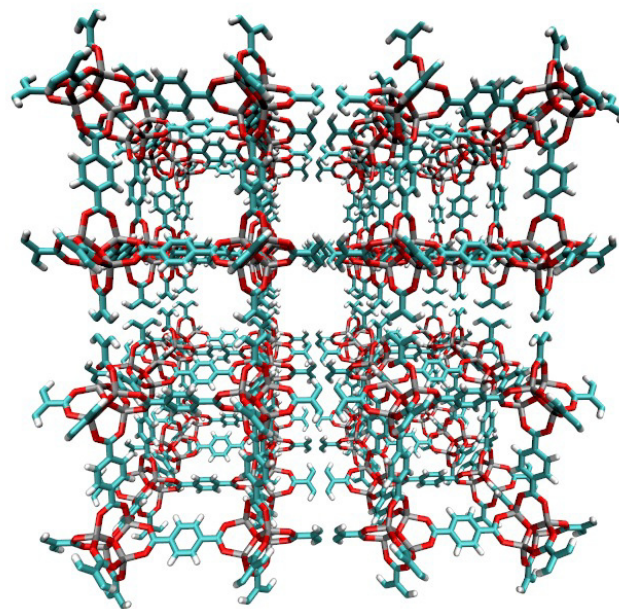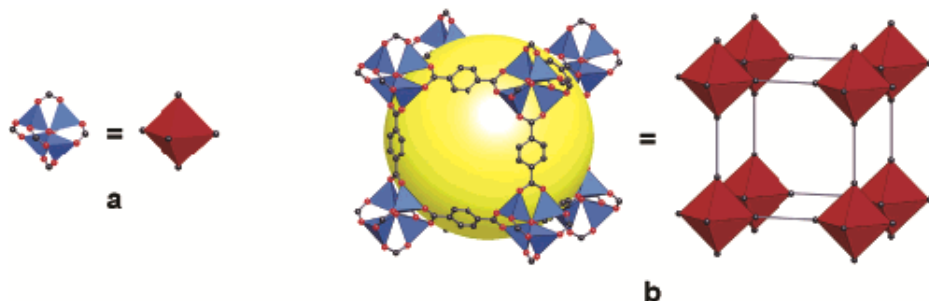
Motivation

understanding the INS **spectra of H_2 in MOF-5**

- wealth of information about excitations of translational and rotational motion of hydrogen - interactions of the guest molecule with the host
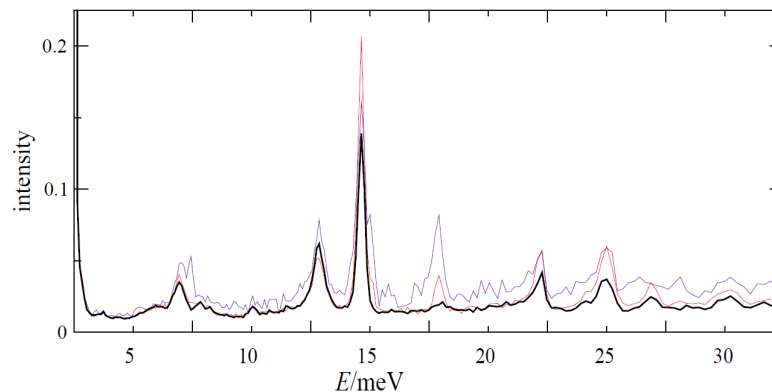
provide valuable insights in exploring the properties of these systems **at the molecular level** - understanding guest-host interactions

$\Rightarrow$ **design of materials with targeted properties, for instance stronger binding energies of H_2**
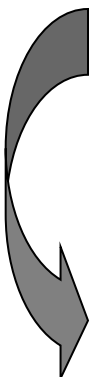
Motivation

calculation of the INS **spectra**

It is essential to have:

i) quantitative description of the **molecule-system potential**

ii) the **methodology** for accurate calculation of the various **spectroscopic observable**

a computer code for **coupled quantum** calculations of the **translational-rotational** energy levels and wave functions of a polyatomic molecule which is confined in (or bounded to) a much heavier entity

Los Alamos
NATIONAL LABORATORY
EST. 1943

Coupled translational rotational problem

5D T-R Hamiltonian:

$$H = -\frac{\hbar}{2m}\left(\frac{\partial^2}{\partial x^2} + \frac{\partial^2}{\partial y^2} + \frac{\partial^2}{\partial z^2}\right) + B\mathbf{j}^2 + V(x,y,z,\theta,\phi)$$

Basis in the angular coordinates – modified spherical harmonics

$$|jm\rangle = \overline{Y}_{jm}(\mathbf{\Omega}) = (-1)^m P_{j,m}(\theta) F_m(\phi) \qquad F_m(\phi) = \begin{cases} \pi^{-1/2}\cos(m\phi), & m > 0, \\ (2\pi)^{-1/2}, & m = 0, \\ \pi^{-1/2}\sin(m\phi), & m < 0. \end{cases}$$

I. Matanović et al., J Chem. Phys. 131, 224308 (2009)

Coupled translational rotational problem

5D T-R Hamiltonian:

$$H = -\frac{\hbar}{2m}\left(\frac{\partial^2}{\partial x^2} + \frac{\partial^2}{\partial y^2} + \frac{\partial^2}{\partial z^2}\right) + B\mathbf{j}^2 + V(x,y,z,\theta,\phi)$$

Basis in the *x,y,z* coordinates – contraction scheme

$$\left|\Phi_t^{xyz}\right\rangle = \sum_{q(\alpha\beta\gamma)=1}^{N_{xyz}} {}^{3D}C_{q(\alpha\beta\gamma),t}^{xyz}|X_\alpha\rangle|Y_\beta\rangle|Z_\gamma\rangle,$$

$$^{3D}h^{xyz}\left|\Phi_t^{xyz}\right\rangle = {}^{3D}\epsilon_t^{xyz}\left|\Phi_t^{xyz}\right\rangle$$

$$^{3D}h^{xyz} = -\frac{\hbar^2}{2m}\left(\frac{\partial^2}{\partial x^2} + \frac{\partial^2}{\partial y^2} + \frac{\partial^2}{\partial z^2}\right) + \overline{V}(x,y,z) \qquad \overline{V}(x,y,z) = \frac{1}{4\pi}\int V(x,y,z,\mathbf{\Omega})d\mathbf{\Omega}$$

I. Matanović et al., J Chem. Phys. 131, 224308 (2009)

U N C L A S S I F I E D

MOF-5: potential

- analytical form

- ab initio
  MP2/def2-TZVP level

$$V = V_{ES} + V_{LJ} + V_{pol}$$
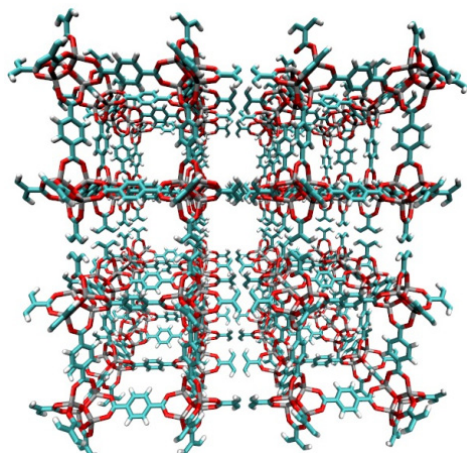
J. L. Belof, A. C. Stern and B. Space, J. Phys. Chem. C. **2009**, 113, 9116.
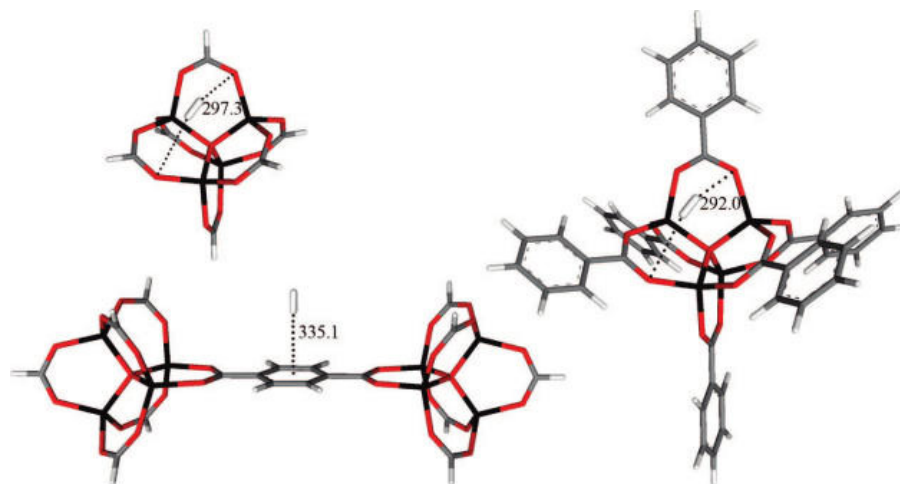
K. Sillar, A. Hofmann, J. Sauer, JACS **2009**, 131, 4143

Los Alamos
NATIONAL LABORATORY
EST.1943

U N C L A S S I F I E D

Slide 44

Operated by Los Alamos National Security, LLC for the U.S. Department of Energy's NNSA

NNSA

MOF-5: binding energies

- four binding sites: 4 α-, 4 β-, 12 γ-sites per Zn_4O unit

	analytical PES	ab initio PES
α - site:	-66.6 meV	-82.9 meV
γ - site:	-65.5 meV	-53.9 meV
β - site:	-53.8 meV	-47.7 meV
δ - site:	-37.8 meV	-52.9 meV

exp: $\alpha-\text{site} \gg \gamma-\text{site} > \beta\text{-site} > \delta\text{-site}$
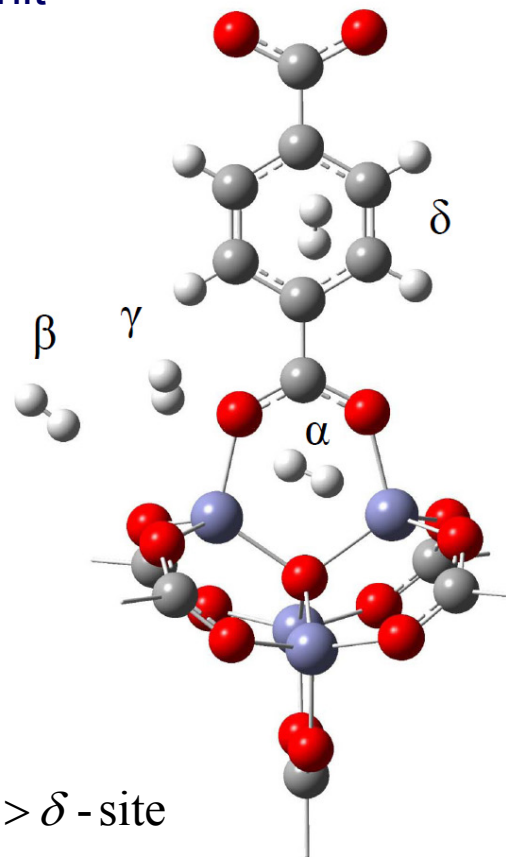
MOF-5: rotational potential

- analytical PES
- ab initio PES

α - site
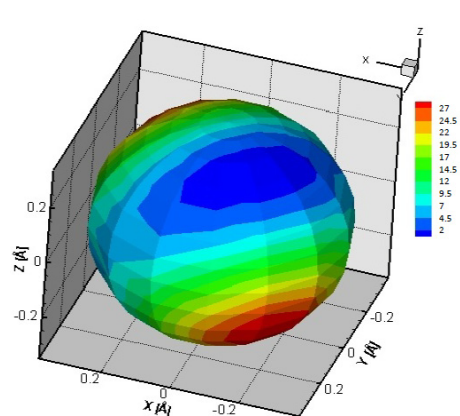
H_2-O_{MOF5} distance: 3.7 Å
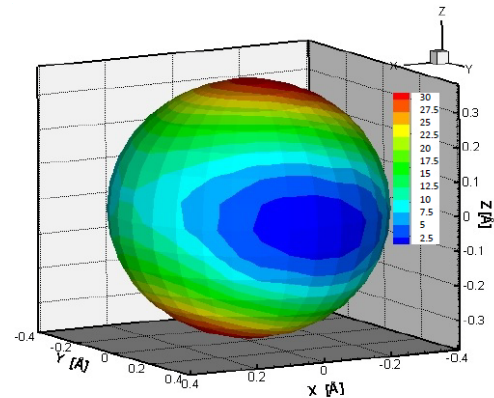
H_2-O_{MOF5} distance: 3.6 Å

γ - site
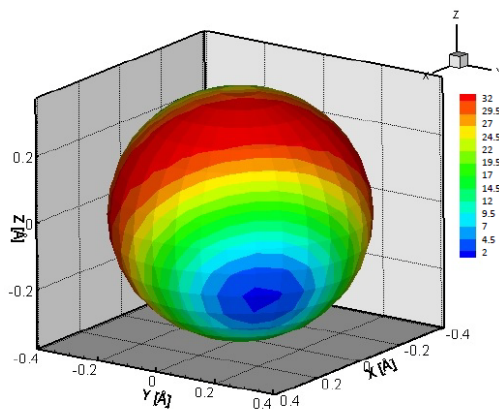
H_2-Zn_{MOF5} distance: 3.9 Å
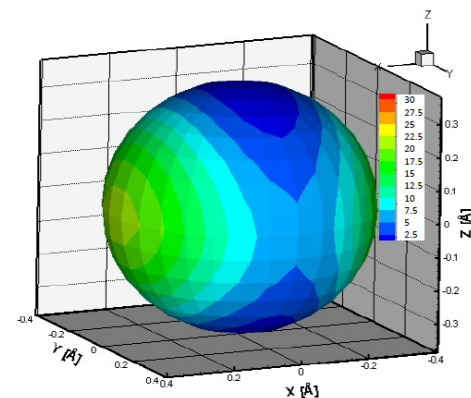
H_2-Zn_{MOF5} distance: 4.1 Å

MOF-5: translational-rotational potential
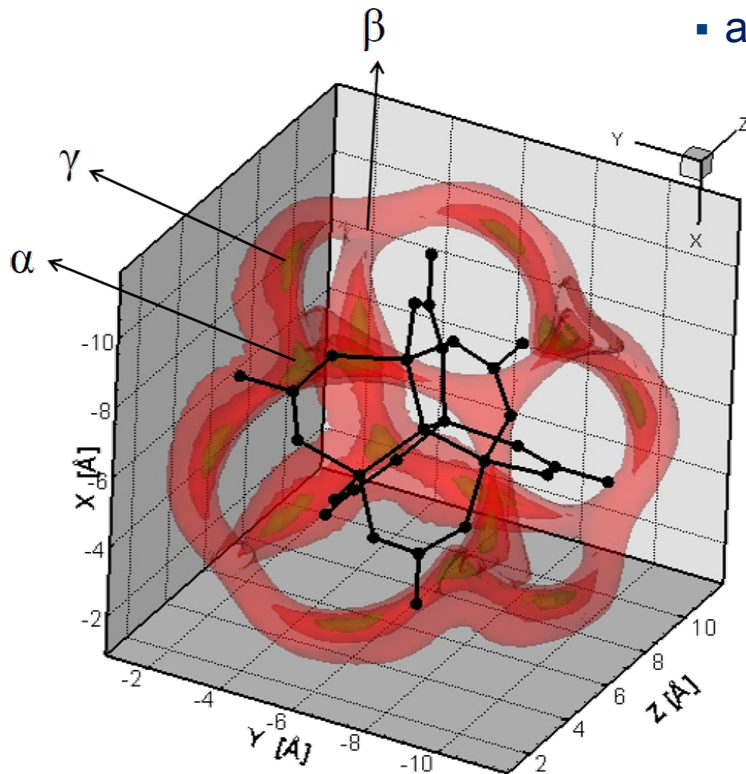
- analytical PES

Figure. 3D isosurfaces at -62, -56 and -44 meV for the 5D analytical PES of H_2 in MOF-5
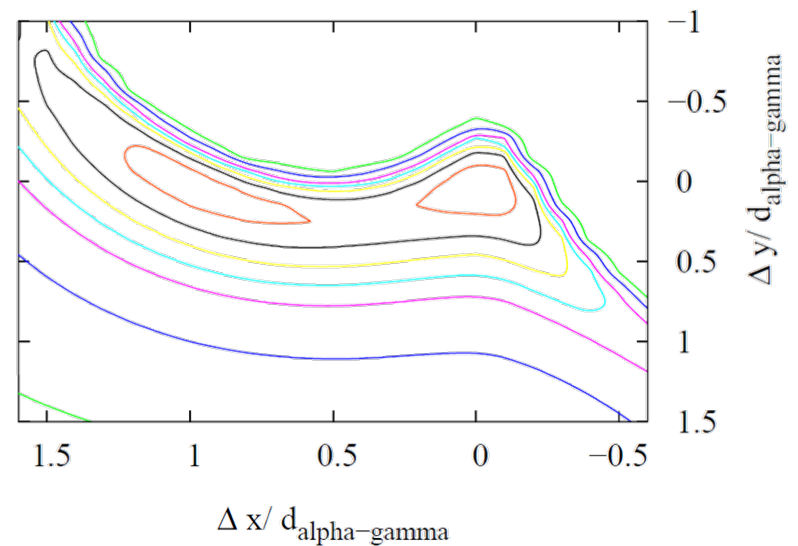
Figure. 2D cut through the potential connecting α- and one of the γ-sites, isosurfaces shown at every 6 meV starting from -62 meV

Operated by Los Alamos National Security, LLC for the U.S. Department of Energy's NNSA

INS spectra: Translation-rotational problem
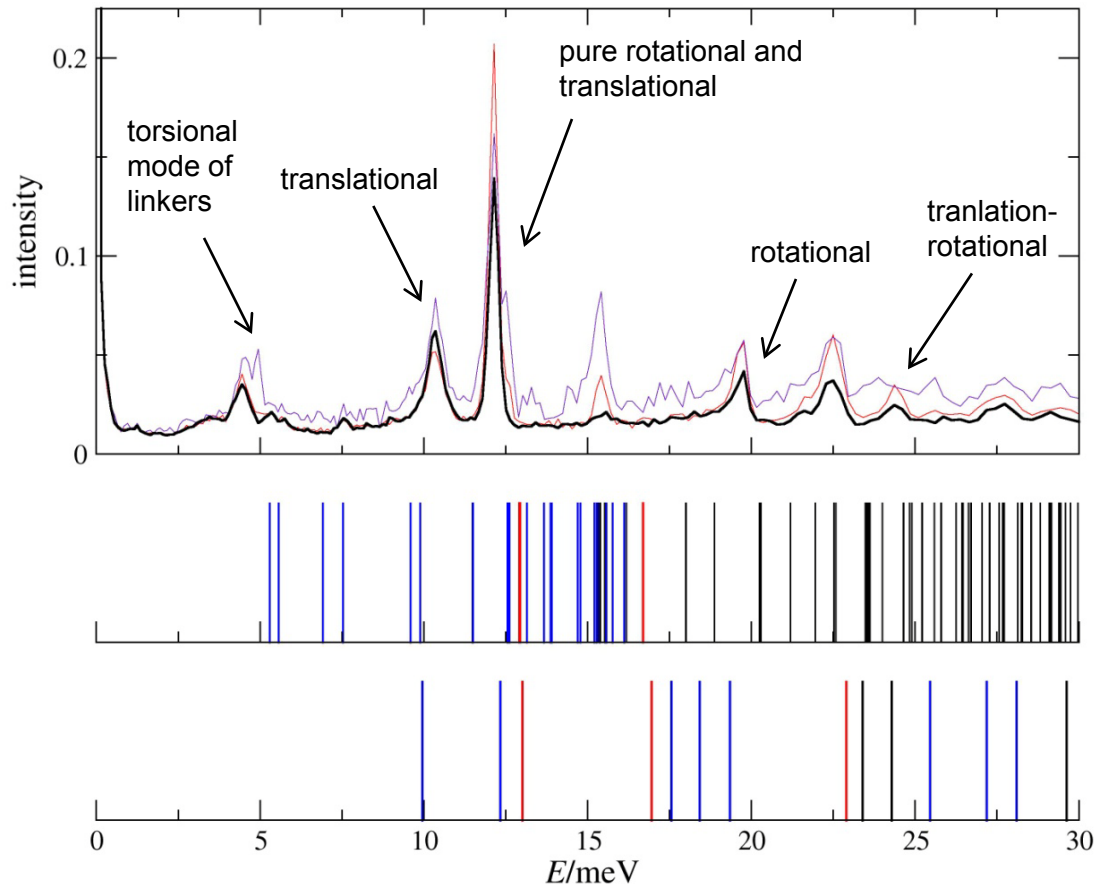
1 H_2 moving in α- and γ- sites

1 H_2 moving in α-site with γ-sites occupied
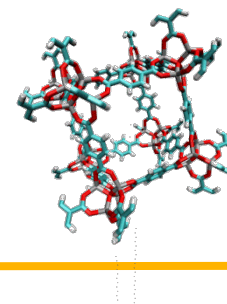
Conclusions

- small barrier between α- and three surrounding γ-sites in MOF-5 on analytical PES by Belof et al.
  low-lying translationally excited states extensively delocalized

- comparison with INS spectra implies that the actual degree of localization in the α-site is greater than indicated by the PES

- INS spectra assigned, intensities needed for more extensive assignment – M. Xu et al Phys. Rev. B 84, 195445(2011)

- PESs that accounts for bulk properties (adsorption isotherms) might not correctly describe the interactions with the host on the molecular level – further improvements needed to obtain spectroscopic observables

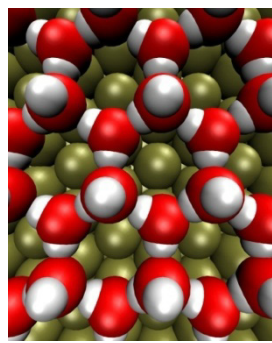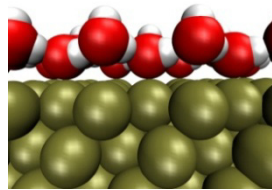# Acknowledgements

Thank you for you attention
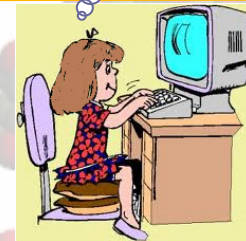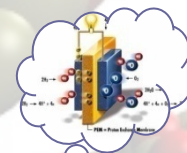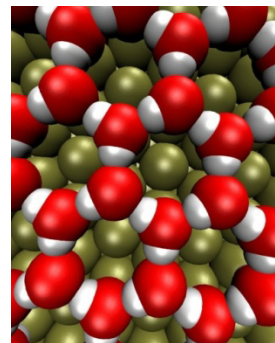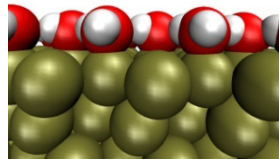
Different states of the metal surface

water layer 1
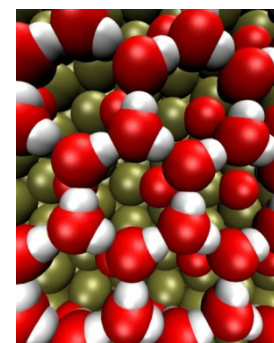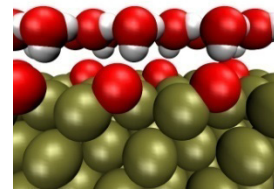
2/3 coverage
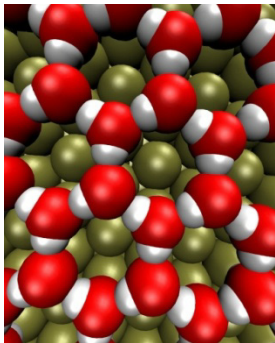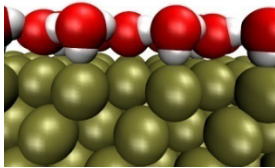
water layer 2
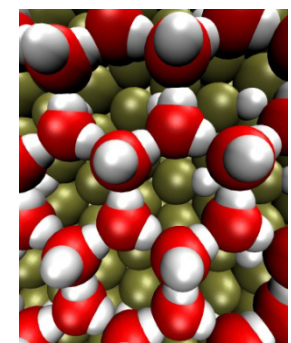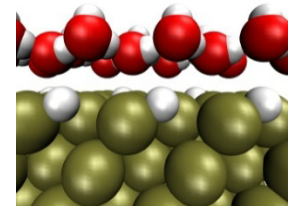
2/3 coverage

OH + water

1/3 coverage

O + water

1/3 coverage

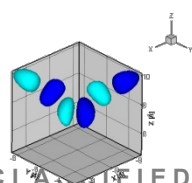H + water

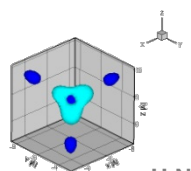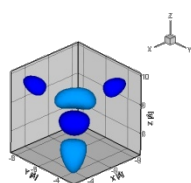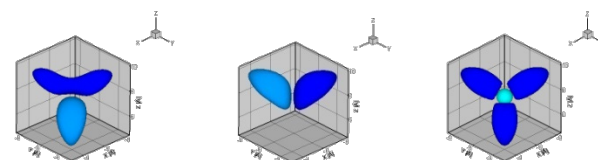1/3 coverage

translation- rotation problem

- rotational problem in separate wells

n	alpha /meV	gamma /meV
0	0.0	0.0
1	10.8	7.5
2	13.3	20.2
3	22.6	21.1
4	40.1	42.0
5	40.1	42.4
6	46.8	43.2
7	48.6	52.3
8	51.9	52.3

- translation - rotational problem (ZPE=218 cm^{-1} / 2.6 kJ mol^{-1})

n	ΔE/ meV	type of excitation
0	0.0	
1	5.3 (2)	translational
3	5.6	translational
4	6.9 (2)	translational
6	7.5	translational
7	9.6 (2)	translational
9	9.9	translational
10	11.5(2)	translational
11	12.5 (3)	translational
16	12.91	rotational, j=1
17	12.94	rotational, j=1
35	16.7	rotational, j=1

lower three translational excitations

Los Alamos
NATIONAL LABORATORY
EST. 1943

U N C L A S S I F I E D

Slide 52

Operated by Los Alamos National Security, LLC for the U.S. Department of Energy's NNSA